

## Chapter

# Vacuum Microwave Sources of Electromagnetic Radiation

*Gennadiy Churyumov, Jinghui Qiu and Nannan Wang*

## Abstract

This chapter contains new simulation results concerning the physical foundations of how microwave tubes operate based on Cherenkov's mechanism of radiation (interaction with slow electromagnetic wave) and some experimental results connected with improving the output characteristics of the magnetrons (a mm band surface wave magnetron and a magnetron with two RF outputs of energy), as well as results of computer modeling of a 320-GHz band traveling wave tube (TWT). The results of analytical calculations and computer modeling, a phase bunching process in the mm band surface wave magnetron, are considered. It is shown that the process of phase focusing has two features associated with a concentration of RF wave energy close to the vanes of an anode block and higher electron hub of a space charge as compared to the classical magnetrons. The features and examples of practical application of the magnetron with two RF outputs of energy are presented. It is shown that the main advantage of the magnetrons is its extended functionalities (for example, possibility of frequency tuning including electronic tuning of a frequency from a pulse to pulse). The presented materials will be of interest not only for starting researchers but also for those who have microwave tube experience.

**Keywords:** Cherenkov's radiation, electromagnetic field, electron beam, magnetron, TWT, frequency tuning, millimeter range, terahertz range

## 1. Introduction

The applications of electromagnetic fields are of great importance in such areas as radar and navigation, communications, information and communication technologies, industry and agriculture, medicine, etc.

It is the interaction of moving charged particles (for example, electrons) with the electromagnetic field that is the cornerstone of electromagnetic phenomena. It is known that the electron moving rectilinearly and evenly with constant speed does not radiate. Moreover, the electromagnetic field, which exists around particle, moves together with particle at the same speed, and its properties remain invariable. If the nature of movement of a particle and/or its speed changes, for example, the trajectory of movement becomes curvilinear or the electron begins to move unevenly (turns to be accelerated or slowed down), the state of its own electromagnetic field also changes. As a result, there arises a free electromagnetic field, i.e., electromagnetic radiation (EMR), which has wave nature and freely advances in the environment in the form of electromagnetic wave. Depending on the existing conditions of its propagation (or accumulation of electromagnetic energy), which are

determined by the properties of the medium (for example, features of the spatial configuration of periodic waveguide and resonant electrodynamic structures) as well as the character of movement trajectories of electrons in an electron beam, there might exist the EMR different types.

The following types of radiation are known: Cherenkov's radiation (interaction with slowed-down waves), transient and diffraction radiations (or Smith-Pascrell's radiation as applied to optical band), and bremsstrahlung and magnetodeceleration radiation (while having a magnetic field), as well as its versions: synchrotron or undulator radiation (for a relativistic case) and cyclotron radiation (for a case of the movement of nonrelativistic particles) [1–7]. The analysis reveals that various mechanisms of the radiations have both common and specific features of their occurrence. It is also necessary to note that the existence of one dominating type of radiation may result in the interference of several types of radiation under certain conditions [8]. As a result, the output parameters of a microwave source will depend on the fact how efficiently the conditions of electron interaction will be correlated with an electromagnetic field from the viewpoint of conversion efficiency of the energy, being reserved in an electronic flow, into electromagnetic energy, and how fully and correctly the requirements to the devices distributing and accumulating an electromagnetic field (periodic and resonator electrodynamic structures) are formulated.

Studying the features of physics of the electromagnetic radiations has led to producing various microwave vacuum tubes in the wide range of frequencies [9]. Considerable recent attention has been focused on creating microwave sources in a short-wave part of millimeter (0.1–0.3 THz) and terahertz (0.3–3.0 THz) ranges. It is known that the absolute advantage of terahertz range is the broad band of frequencies, as well as the ability to penetrate through opaque media, including metals, organic materials, etc. This property positively distinguishes it from ionizing radiation (for example, X-rays) while opening wide perspectives to diagnose a variety of diseases in medicine [10].

The scheme of practical mastering of a short-wave part of a spectrum of electromagnetic oscillations is shown in **Figure 1**.

It is evident nowadays that the lack of the microwave vacuum devices with continuous power output from a few watts to tens and more watts in this part of the electromagnetic spectrum restricts the opportunities of further development and improvement of technologies in such areas as spectroscopy, radio astronomy, space, and biochemical research, as well as producing a new generation of information and communication systems. Besides the development of this frequency range will allow intensifying safety control (search and detection of explosives, remote identification of chemical substances) to exercise production quality control of finished goods (checking packages of medical products, etc.). The application of relativistic tubes (for example, the relativistic magnetrons or the fast-wave devices like free-electron lasers or gyrotrons) for solving the above-mentioned

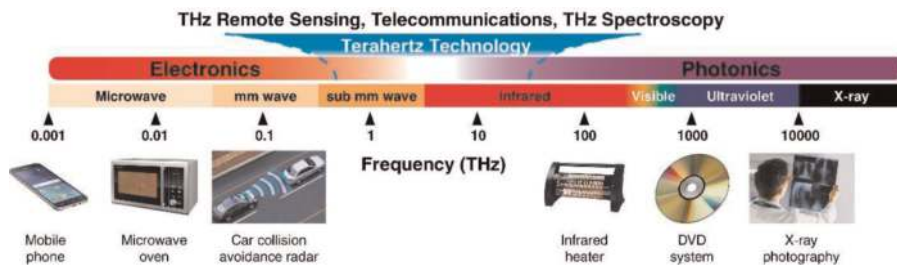


**Figure 1.**  
*The scale of electromagnetic waves and areas of their application.*

problems allows providing the needed levels of output power in this range. However, these devices possess large mass-dimensional characteristics and require for operating the high values of voltages and strong magnetic fields. In this regard, producing effective and compact microwave sources of electromagnetic oscillations in this frequency range seems to be much more attractive with the help of miniaturizing the constructions of the classical microwave tubes possessing Cherenkov's radiation mechanism.

The present chapter deals with vistas of developing the microwave sources of electromagnetic oscillations (the magnetron and the O-type TWT) whose operation is based on the interaction of an electron beam with the slowed-down electromagnetic wave of electrodynamic structure ( $\nu_{ph} < c$ , where  $\nu_{ph}$  is the phase velocity of electromagnetic wave and  $c$  is the light speed), i.e., there exists Cherenkov's radiation mechanism.

## **2. Microwave tubes with Cherenkov's radiation mechanism**

### **2.1 General subjects**

Microwave sources operating on basis of Cherenkov's radiation are a wide class of microwave tubes, including the magnetrons, backward-wave tubes (BWTs), resonant TWTs, and orotron [9]. As for now, microwave sources with Cherenkov's interaction have allowed to reach the maximum levels of peak capacity  $\sim 3$  GW in the 3-cm range of wavelength and more than 5 GW in the 8-cm range at a pulse duration of 1–10 nanoseconds including the generation of ultrashort pulses of electromagnetic radiation (the effect of superradiation) [11]. Let us consider the development of these tubes on the example of their most famous representatives, which are magnetrons and TWTs.

### **2.2 Magnetron**

Historically, the first microwave tube whose operation is based on Cherenkov's interaction was a magnetron [12]. The successful combination of properties of a multimode oscillating system of the magnetron and electronic processes occurring in its interaction space has allowed the magnetron to become one of the most effective microwave generators [13, 14]. The constructions of magnetrons developed nowadays generate electromagnetic oscillations in the frequency range from 300 MHz to 300 GHz. The output power of continuous magnetrons ranges from a few fractions of a watt to several tens of kilowatts, and the pulsed magnetrons generate the electromagnetic oscillations with output power from 10 W to 20 MW. Both pulsed and continuous magnetrons are widely used in different ground-based and on-board electronic systems, industrial and microwave household heating systems, physical experiments for plasma heating, and the acceleration of charged particles, as well as in the phased antenna grids and space systems of solar energy conversion to direct current energy (the system of wireless energy transmission to the earth). The miniaturization of the magnetron construction has allowed to reduce their weight to 100 g at the pulsed power of 1 kW and the efficiency of which achieves about 50% that is quite competitive with the best samples of modern transistor oscillators [10, 13–20].

Concerning the existing trends of investigations, it is necessary to emphasize the problems of improvement of the cathode (emitter) operation of magnetrons. It is found (see, e.g., [13, 14, 21]) that the changes and instability of the cathode

emission characteristics influence considerably the frequency stability of the magnetron. On the other hand, the disorder in the operation mode of the cathode connected with its overheat leads to essential reduction of durability of the cathode and the cathode node as a whole. In this regard, it is of great interest to study the problem of excess electronic and/or ionic bombing of the cathode and to clarify the role of turbulence of a cathode electronic cloud in the course of secondary-emission multiplication of an electronic beam [22, 23]. In order to improve the magnetron operation, there conducted active investigations of new effective cathode materials and cathode node constructions, providing high durability and emission stability. It especially concerns investigations connected with applying the cold secondary-emission cathodes providing virtually instant readiness and nonfilament (“cold”) start of magnetrons [22, 24–28].

The scope of magnetrons continues to expand constantly that is primarily caused by their advantages such as high electronic efficiency (more than 80%), relatively low voltages (in particular, anode voltage), the high relation of power output level to the weight of the tube, the compactness of construction, the simplicity of production, and comparatively low cost [10, 15]. However, such drawbacks of magnetrons as the low stability of frequency, the increased noise levels, and spurious oscillations require carrying out additional investigations and analyzing the ways for improving its output characteristics, in particular, in a short-wave part of a millimeter range. Solving mentioned above problems will allow to increase competitiveness of magnetrons and to expand their functionality in comparison with other microwave tubes, such as one-beam and multibeam klystrons, klystrons, complexified microwave sources on the basis of “the solid-state generator and TWT” chains, etc. [10, 13, 14, 21, 22, 24, 25].

### *2.2.1 The surface wave magnetrons*

The state-of-the-art evolution of magnetrons is associated with increasing the frequency (phase) stability and rising the lifetime, as well as enhancing reliability due to an application of the cold cathodes [21, 24, 26–28]. In particular, there is a significant interest in the development of magnetrons in the millimeter range. These magnetrons can be applied in radar systems [29]. Among possible designs of similar magnetrons, it is necessary to select the magnetrons working on higher space harmonics (for example, by using as operating a first negative ( $-1$ ) space harmonic or an oscillation does not  $-\pi$  mode [30]). The magnetrons operating in such modes are named the surface wave magnetrons [30, 33]. According to the approach described in [32], a method has been developed to calculate the parameters and the operation modes. It is necessary to note that a major feature concerning to the application of the surface wave magnetron is associated with the generation of electromagnetic waves in the millimeter range at a considerably low magnetic fields and increased sizes of an interaction space. The prototypes of the surface wave magnetrons have been built. The prototypes operate at the  $\frac{\pi}{2}$  – mode, and they provide the following output parameters: wavelength band from 1.25 mm up to 6.8 mm, a level output pulsed power from 1 up to 150 kW, and efficiencies 0.8–20% [31].

In spite of the intensive research over the years and getting experimental results including the constructions of the surface wave magnetrons, up to now, we have no necessary and full information about physical processes occurring in the interaction space of given magnetrons. Therefore, for studying and understanding the features of a mechanism of nonlinear interaction into an interaction space of the magnetron, it is necessary to carry out additional computer modeling, a phase

bunching process of an electron beam under its interaction with surface wave by using the Particle-in-Cell Method.

For studying, we used the design of a 3-mm range magnetron. Schematically, this design presents in **Figure 2**. The essential geometry sizes of an interaction space of this magnetron are presented in **Table 1**. As the operation mode, the mode other than the  $\pi$ - mode was taken, namely, the oscillation  $\frac{\pi}{2}$ - mode. As cathode of the magnetron, an indirectly heated oxide cathode, which produced an emission current density of  $\sim 2.0 \text{ A/sm}^2$ , was used [37].

For computer modeling, we used the 2-D mathematical model of the magnetron described in [34]. The basis of this model is the self-consistent set of equations including the motion equation, the equation of excitation, and Poisson's equation for calculation of space charge forces.

As already mentioned above, the theoretical basis of the surface wave magnetrons was described in the works [30–32]. It is necessary to note that the distinctive feature of electron-wave interaction in given magnetrons (for example, as distinguished from the classical magnetrons [14], using the  $\pi$ - mode as the operation one) is the distribution of an electromagnetic wave in the neighborhood of a surface of the RF structure and its interaction with electrons on a top of the space charge hub. In order to understand the mechanism of interaction of an electromagnetic field with an re-entrant electron beam, it is very important to define the features of the radial and azimuthal distributions of the electromagnetic wave in an interaction space (between a cathode and inside surface of an anode block (see **Figure 2**), as well as to provide clearer understanding about behavior of electrons and their motion trajectories.

An interaction space of the magnetron is shown in **Figure 2**, schematically. In order to determine the electromagnetic field in the resonance RF structure (anode

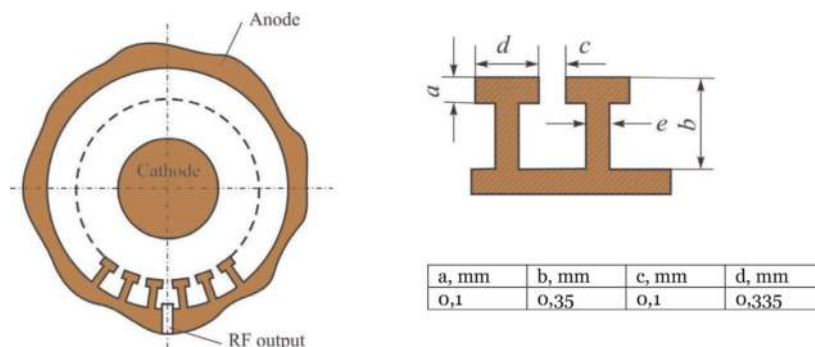


**Figure 2.**  
 Schematically image of a surface wave magnetron.

Parameters	Symbol	Unit	Value
1. Frequency	$f$	GHz	9.2
2. Cathode radius	$r_c$	mm	0.85
3. Anode block radius	$r_a$	mm	1.665
4. Anode block height	$h$	mm	4.0
5. Resonators number	$N$	mm	24

**Table 1.**  
 The main parameters of surface wave magnetron.

block), we used the decision obtained from Maxwell's equations for free space without charged particles [14]. As a result, the expressions for components electromagnetic field in the interaction space may be written as

$$E_\phi(r, \phi) = E_m \frac{N\theta}{\pi} \sum_{m=-\infty}^{\infty} \left( \frac{\sin \gamma\theta}{\gamma\theta} \right) \times \frac{Z_\gamma'(kr)}{Z_\gamma'(kr_a)} \cdot e^{j\gamma r\phi}; \quad (1)$$

$$E_r(r, \phi) = -jE_m \frac{N\theta}{\pi kr} \sum_{m=-\infty}^{\infty} \gamma \cdot \frac{\sin \gamma\theta}{\gamma\theta} \times \frac{Z_\gamma(kr)}{Z_\gamma'(kr_a)} \cdot e^{j\gamma r\phi}, \quad (2)$$

where  $k = 2\pi/\lambda$  is the propagation factor in free space;  $\lambda = c/f$  the wavelength of the magnetron;  $2\theta$ —the angle subtended by a space between segments of the anode block;

$$Z_\gamma(kr) = J_\gamma(kr) - \frac{J_\gamma'(kr)}{N_\gamma'(kr_a)} \cdot N_\gamma(kr) \quad (3)$$

and

$$Z_\gamma'(kr) = J_\gamma'(kr) - \frac{J_\gamma'(kr_c)}{N_\gamma'(kr_a)} \cdot N_\gamma'(kr) \quad (4)$$

are the combinations of the well-known Bessel  $J_\gamma(kr)$  and Neumann  $N_\gamma(kr)$  functions;  $\gamma$  is zero or any positive or negative integer.

In the expressions of Eqs. (1) and (2), we have the ratio of  $\frac{Z_\gamma'(kr)}{Z_\gamma'(kr_a)}$  and  $\frac{\gamma Z_\gamma'(kr)}{kr Z_\gamma'(kr_a)}$ , which are the structure functions of the electromagnetic field. From these expressions, we have seen that their values depend on a radius-vector  $\vec{r}$  and bring about changing the magnitude of the  $\gamma$ -th mode in the radial direction of the interaction space. It is necessary to note that when  $kr_a \ll \gamma$  (so-called long-wave approximation), the expressions can be simplified as [14]:

$$\Psi_r^\gamma(r) = \frac{Z_\gamma'(kr)}{Z_\gamma'(kr_a)} \approx \left( \frac{r}{r_a} \right)^{\gamma-1} \cdot \left[ \frac{1 - \left( \frac{r_c}{r} \right)^{2\gamma}}{1 - \left( \frac{r_c}{r_a} \right)^{2\gamma}} \right]; \quad (5)$$

and

$$\Psi_\phi^\gamma(r) = \frac{\gamma Z_\gamma'(kr)}{kr Z_\gamma'(kr_a)} \approx \left( \frac{r}{r_c} \right)^{\gamma-1} \cdot \left[ \frac{1 + \left( \frac{r_c}{r} \right)^{2\gamma}}{1 - \left( \frac{r_c}{r_a} \right)^{2\gamma}} \right]. \quad (6)$$

Thus, the expressions obtained for components of an electromagnetic field of (1) and (2) in terms of (5) and (6) allow getting an electromagnetic field for the  $\gamma$  - mode of a cold resonance anode block of a magnetron as

$$\vec{E}(\vec{r}, t) = \text{Re} \left\{ \vec{E}(\vec{r}) \cdot e^{-j\omega_\gamma t} \right\}, \quad (7)$$

where  $\vec{E}(\vec{r}) = E_r(r, \phi) \cdot \vec{r}^0 + E_\phi(r, \phi) \cdot \vec{\phi}^0$ ,  $\omega_\gamma = \omega_\gamma' - j\omega_\gamma''$ —the complex cold frequency of the  $\gamma$  - mode;  $\omega_\gamma' = 2\pi \cdot f$ —the angular frequency of the  $\gamma$  - mode;  $\omega_\gamma''$ —the coefficient of attenuation.

Each mode excited in the anode block of the magnetron is characterized by certain distribution of the electromagnetic field and its frequency  $\omega_\gamma = \omega_\gamma'$  in an approximation  $\omega_\gamma'' = 0$ . In the general case, the electromagnetic field in the interaction space is not sinusoidal and may be presented as a sum of the space harmonics, each of which corresponds to the wave rotating with an angular velocity  $\Omega_\gamma$  and containing along the azimuthal length of the interaction space of a magnetron the whole number of the complete periods

$$\gamma = n + mN, \quad (8)$$

where  $n = 0, 1, 2, \dots, N/2$  is the number of the fundamental mode ( $m = 0$ );  $m = \pm 1, \pm 2, \pm 3, \dots$  is the integers corresponding to the high-order space harmonics. It is known (see, example, [13, 14]) that the excitation condition of the resonant system of the magnetron (or so-called a condition synchronism) may be written as

$$\Omega_e = \Omega_\gamma, \quad (9)$$

where  $\Omega_e$  is the angular velocity of rotating electron spokes (or an electron beam closed on itself—re-entrant electron beam). On the other hand, we have an electron cloud, which circles in the interaction space around the cathode [9, 14], i.e., there is an additional condition, which is associated with a re-entrant electron beam and may be written as

$$\gamma = \frac{\omega_\gamma}{\Omega_e}. \quad (10)$$

The fundamental results of theoretical analysis are shown in **Figure 3**. The comparison of the radial functional dependences of the structural functions, Eq. (5) and Eq. (6), for two cases at using the higher space harmonics (for example, space harmonic—1 and  $\gamma = 18$ , curve 1) and at a classical  $\pi$ -mode ( $m = 0$  and  $\gamma = 12$ , curve 2), shows that in the first case for effective interaction between electrons and electromagnetic wave, it is necessary to form the electronic hub having a height more than 0.85.

The trajectories of moving electrons as a result of interacting with electromagnetic field of the  $(-1)$  space harmonic are shown in **Figure 4**. Besides, here for comparison, we can see the trajectories of the electrons in the static mode of magnetron operation (dashed curves). It is seen that the phase focusing of the electron beam takes place in the range of the proper phases of the RF wave. In the range of the improper phases, we observe the multiplication secondary electrons process, increasing the density of space charge in the electron hub.

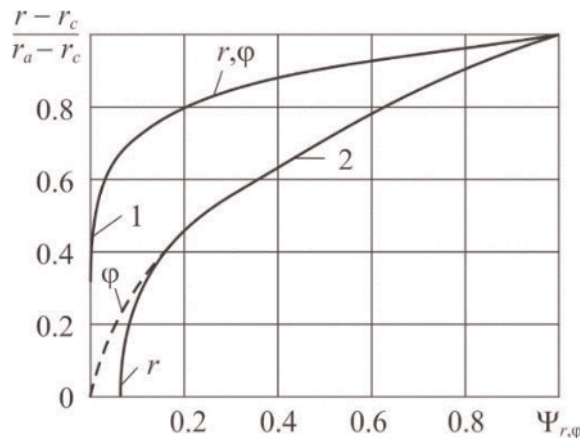


**Figure 3.**  
 The radial distributions of the structural functions.

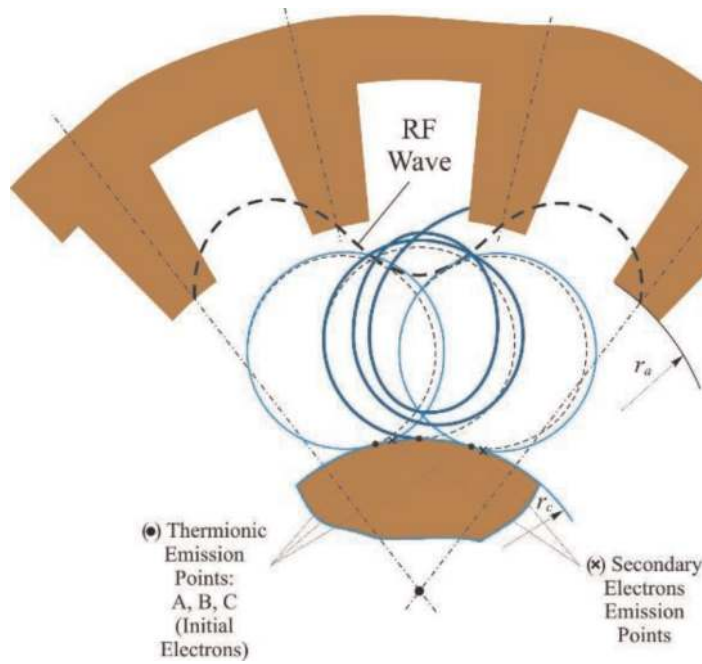


**Figure 4.**  
The trajectories of electrons in the interaction space [35].

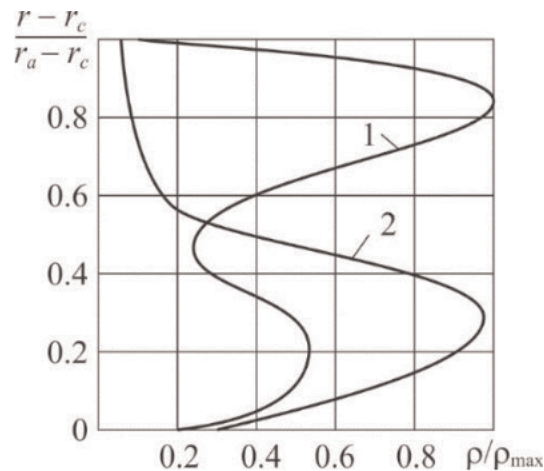


**Figure 5.**  
The radial distributions of space charge density in the interaction spaces of the surface wave magnetron (1) and the classical ( $\pi$ -mode) magnetron (2).

**Figure 5** shows the steady-state radial distributions of space charge densities in the interaction spaces of a surface wave magnetron and a classical magnetron. As can be seen, there is a fundamental difference between the two processes of the phase focusing. It is associated with available maximum of the space charge density in the immediate neighborhood of the surface of the RF structure (anode block). The availability of a second maximum of the space charge density allows the double stream state to be established in the electron hub.

It is also important to note that the operation mode on higher spatial harmonics applied in the magnetron, namely on  $-1$  spatial harmonic or  $\frac{\pi}{2}$ -mode of oscillation, was rather successfully used for creating a relativistic prototype of the high-power magnetron with pulsed power of  $\sim 1$  MW at the frequency of 37.5 GHz [34].



On the basis of the design of the 3-mm surface wave magnetron, there is a possibility to design the amplifying variant of a new microwave tube. **Figure 6** presents a design of a 3-mm surface wave magnetron amplifier (amplitron). The main difference of the amplitron from magnetron lies in the fact that an anode block of the amplitron is nonresonant slow-wave structure in which an electromagnetic wave propagates from a RF input to a RF output, i.e., in an interaction space of the amplitron, there is a process exchange of electromagnetic energy between a re-entrant electron beam and traveling wave that is propagated from RF input to RF output and then to a matched load.

**Figure 7** shows the experimental dispersion characteristics of a comb-shape slow-wave structure of the 3-mm surface wave amplitron.

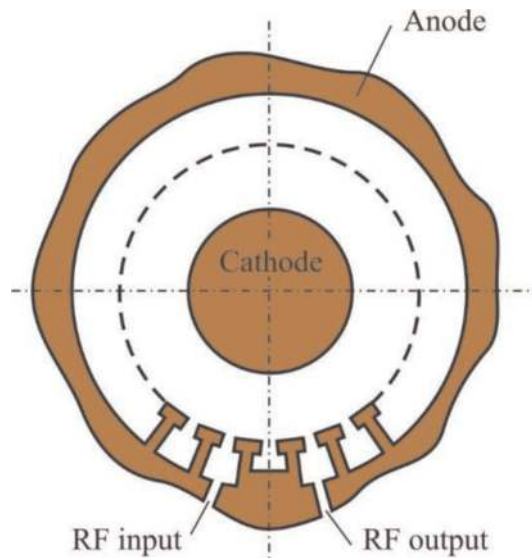


**Figure 6.**  
*A scheme of interaction space of an amplitron.*

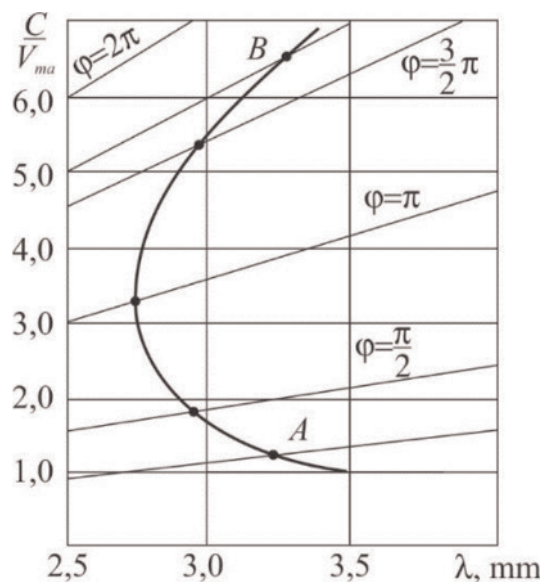


**Figure 7.**  
*A scheme of interaction space of an amplitron.*

### 2.2.2 Magnetrons with two energy outputs

Recently, there have been functional problems of different electronic systems, which became all more complex [15, 16, 18]. In particular, multifrequency radar operating in various frequency ranges for monitoring the clouds and precipitation (meteorological radar) or observing the water area and the movement of vessels in port services are increasingly applied [16]. Wherever such radars are required, there is a great quantity of interfering factors, and the multifrequency systems allow solving these problems. The operation of such radars requires a new functional element base (vacuum tubes) capable to give a functionally simple solution to a problem of multifrequency generation with high-operating characteristics. As an example of the multifrequency generator it can be a magnetron implementing the mode of an electron frequency tuning (including frequency tuning from pulse to pulse) and its application in electronic systems of different functional purpose [35, 36, 38, 39]. The practice shows [see, for example, 38, 39], that in this case in a design of the magnetron we can use two RF outputs of energy: one as active output and other a reactive one which is used for tuning a frequency.

The anode block of the magnetron with different possible variants of arrangement of the second RF output is presented in **Figure 8**. As may be seen, the second RF output of energy can be placed both symmetrically (1') and antisymmetrically (2 и 2') to the active RF output (1'). The main constructional and electrical parameters of the basic design of the magnetron are given in **Table 2**.

Using an existing design method of the magnetrons, described in [41], a code for computer aided design of geometry and electrical parameters of the magnetrons was developed. The computation being made with the help of this code allowed defining all parameters of the magnetron provided that a maximum current from cathode was not more than  $1 \text{ A/sm}^2$ .

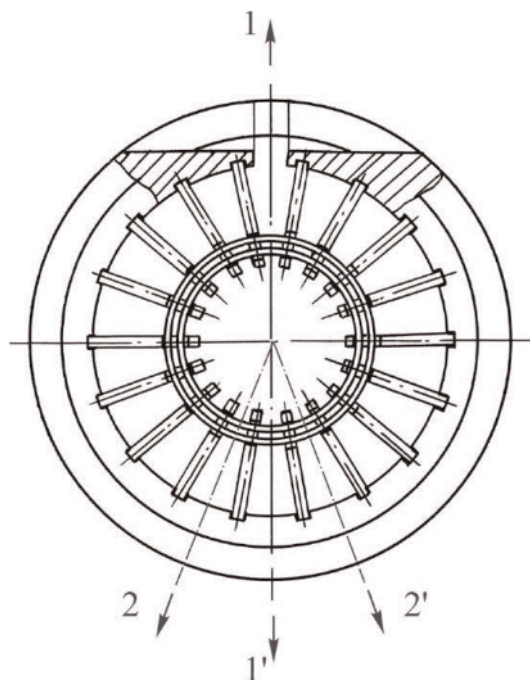


**Figure 8.**  
The possible variants of arrangement of the second RF output of energy.

Parameters	Symbol	Unit	Value
1. Frequency	$f$	GHz	9.42
2. Cathode radius	$r_c$	mm	2.225
3. Anode block radius	$r_a$	mm	3.25
4. Anode block height		mm	7.0
5. Resonators number	$h$	mm	18
6. Anode voltage		kV	7.3

**Table 2.**  
 The parameters of a magnetron.

In order to choose the operation mode of the magnetron and to apply computer modeling using its 3-D mathematical model, it is necessary to carry out the analytical calculations to define the Hull cutoff curve

$$U = 0,022 \cdot r_a^2 \cdot B^2 \cdot \left(1 - \frac{r_c^2}{r_a^2}\right)^2$$

where  $r_c$  and  $r_a$  are the radiuses of the cathode and the anode in sm;  $B$  is the magnetic field, Gs. Also, Hartree's voltage that can be written as

$$U_{Hartree} = U_{\min} \cdot \left[ \frac{2 \cdot B}{B_0} - 1 \right],$$

where

$$U_{\min} = 253 \cdot 10^3 \cdot \left[ \frac{2\pi r_a}{n \cdot \lambda} \right]^2,$$

$$B_0 = \frac{21200}{n \cdot \lambda \cdot \left[1 - (r_c/r_a)^2\right]},$$

$n$  – a mode of oscillation (for  $\pi$ – mode  $n = \frac{N}{2}$ ) and  $\lambda$ – wavelength in a free space.

As illustrated in **Figure 8**, as an example of the electrodynamics system of the basic design of the magnetron, we used an anode block with having the double two-sided straps. We have investigated the electrodynamics of the anode block by applying boundary conditions on an FDTD simulation.

The theoretical dependence of dispersion characteristic of the trapezoidal anode block with double two-sided straps for  $\pi$ – mode ( $n = \frac{N}{2}$ ) and three nearest to the spurious modes ( $n = (\frac{N}{2} \pm 1)$ ,  $(\frac{N}{2} \pm 2)$ , and  $(\frac{N}{2} \pm 3)$ ) is shown in **Figure 9**.

As we can see from **Figure 9**, the separation between the main operative mode ( $\pi$ – mode, when  $n = \frac{N}{2}$ ) and the nearest spurious modes ( $n = (\frac{N}{2} \pm 1)$ ) is more than 2200 MHz. Such separation between the nearest competing modes in the magnetrons allows effectively to solve a problem of the frequency tuning in wide frequency range. On the other hand, for understanding the general situation associated with the influence of the design and axial dimensions of end regions on the shift of resonance frequency of electrodynamics system, it is necessary to carry out an additional calculation and analysis.

**Figure 10** shows a curve of shift of a resonance frequency of the anode block depending on the axial height of the end region between the vanes and end covers of electrodynamics system.

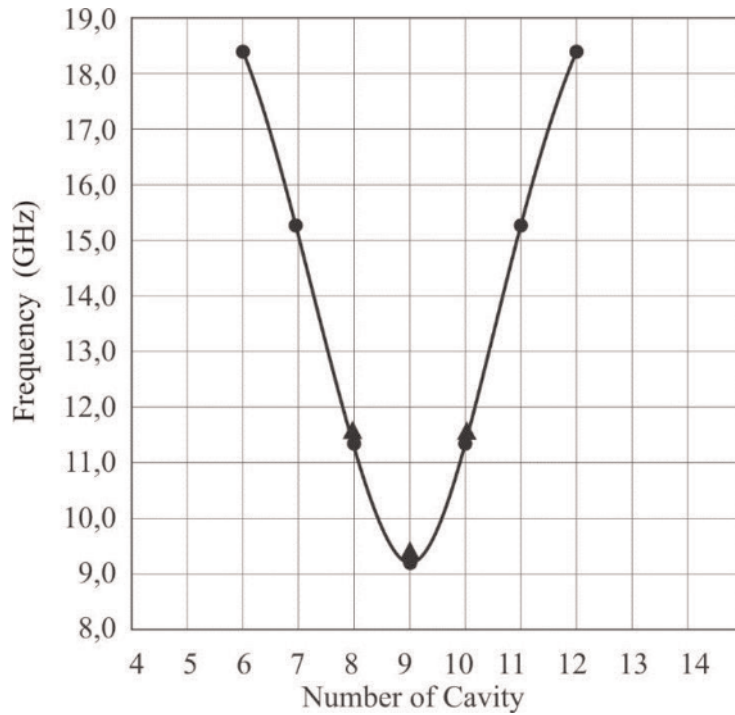


**Figure 9.**  
The results of computer modeling of the dispersion characteristic of an anode block.

An investigation of the electrodynamic parameters (dispersion) of the anode block was carried out experimentally. A panoramic measurer of VSWR of P2–65 type was used in the measurement. By using such approach, we viewed the resonance oscillation on an operating  $\pi$ - mode and nearest to the spurious modes of oscillation when  $n = (\frac{N}{2} \pm 1)$ . The comparison of the theoretical computation with the data of the experiment is presented in **Table 3**.

A general view of the magnetron with two energy output ports is schematically illustrated in **Figure 11**. As may be seen, the active RF output 2 of the magnetron is matched with load 5 and its reactive (passive) RF output of energy 3 is connected with a length of waveguide containing a short-circuiting piston 4. By varying the distance

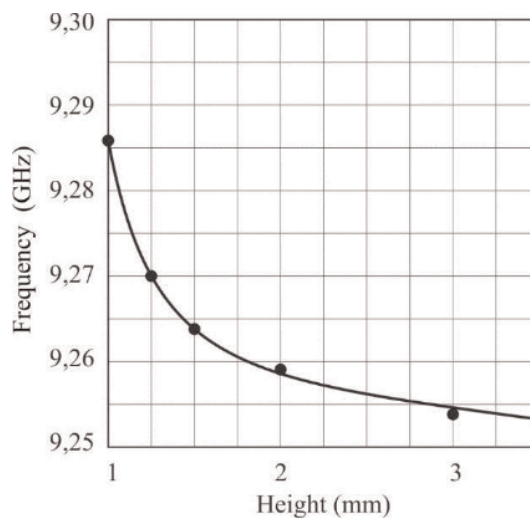


**Figure 10.**  
A resonance frequency of the “cold” anode block as a function of the distance between the vanes and end covers.

Parameters	Theory	Experiment
Frequency of operating mode $n = \frac{N}{2}$ , MHz	9253.47	9230.00
Frequencies of nearest spurious modes $n = (\frac{N}{2} \pm 1)$ , MHz	11470.61 11480.56	11498.00 11828.00

**Table 3.**  
 Comparison theory with data of experiment.

from reactive RF output up to the short-circuiting piston, we are changing the input complex resistance of the waveguide 4 according to the following expression

$$Z_{inp} = jZ_0 \cdot tg \frac{2\pi L}{\lambda_g}, \quad (11)$$

where  $Z_0$ —an input characteristic impedance of a waveguide and  $\lambda_g$ —wavelength into waveguide. As a result, a reactive component of a complex impedance of the anode block of the magnetron is changed and a resonant frequency of the anode block is retuned.

An experimental curve of the frequency tuning for a “cold” anode block of the 3-sm magnetron with two RF outputs of energy is presented in **Figure 12**. As may be seen, changing a length of line circuit (waveguide)  $L$  leads to a periodical changing a resonant frequency of the magnetron with a special period  $\lambda_g/2$ . As this

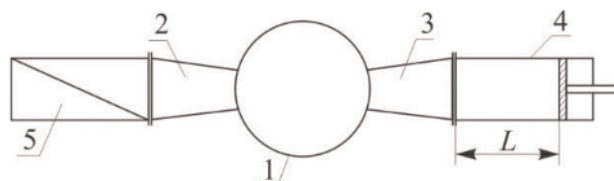


**Figure 11.**  
 Schematic image of a magnetron with two RF outputs of energy. 1—an anode block of the magnetron; 2—an active RF output of energy; 3—a reactive RF output of energy; 4—a waveguide including a short-circuiting piston; 5—a matched load.

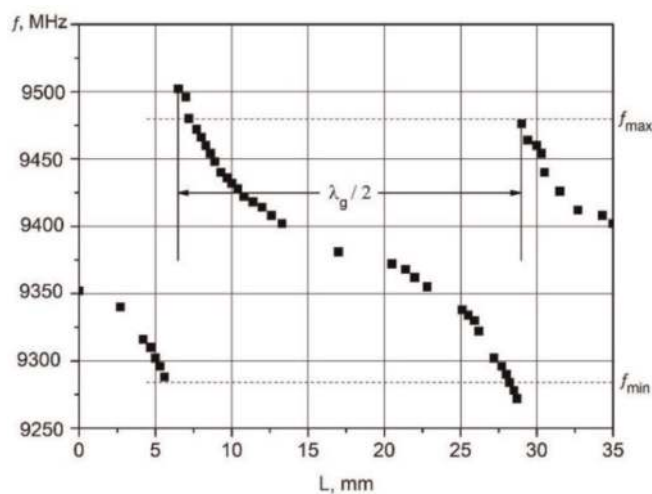


**Figure 12.**  
 Experimental curve of frequency tuning in the X-band magnetron with two RF outputs.

takes place, the full frequency tuning range is exceeded 200 MHz that is sufficient for practical application.

For comparison in **Figure 13**, we present the 3 D images and axial sections of a classical magnetron (a) and a magnetron with two RF outputs of energy (b).

### 2.2.3 Examples of application of a magnetron with two energy outputs

The vistas of developing the magnetrons associated with stabilization of frequency and improvement of its frequency characteristics including its operation in the multifrequency mode and the electronic frequency tuning [21, 35, 36, 38].

A block diagram of a device on basis of the magnetron with two RF energy outputs and realizing a multifrequency mode of an operation with electronic tuning of a frequency from pulse to pulse is shown in **Figure 14**.

As may be seen, the given block diagram of the pulsed magnetron generator includes a magnetron with two RF outputs: active – 1 and passive – 2, as well as modulator – 4, which is synchronized with a pulsed power supply 7 for commutation of the p-i-n diodes  $D_1$  and  $D_2$  of an electronic switch 5. The microwave energy generated a magnetron, on the one hand, is consumed by a matched load 2 via the active RF output 1 and on the other hand is passed the reactive RF output 3 and entered on a microwave switch 5. The microwave switch is a device, which has one input and several outputs each has a load in short-circuit waveguide form length of

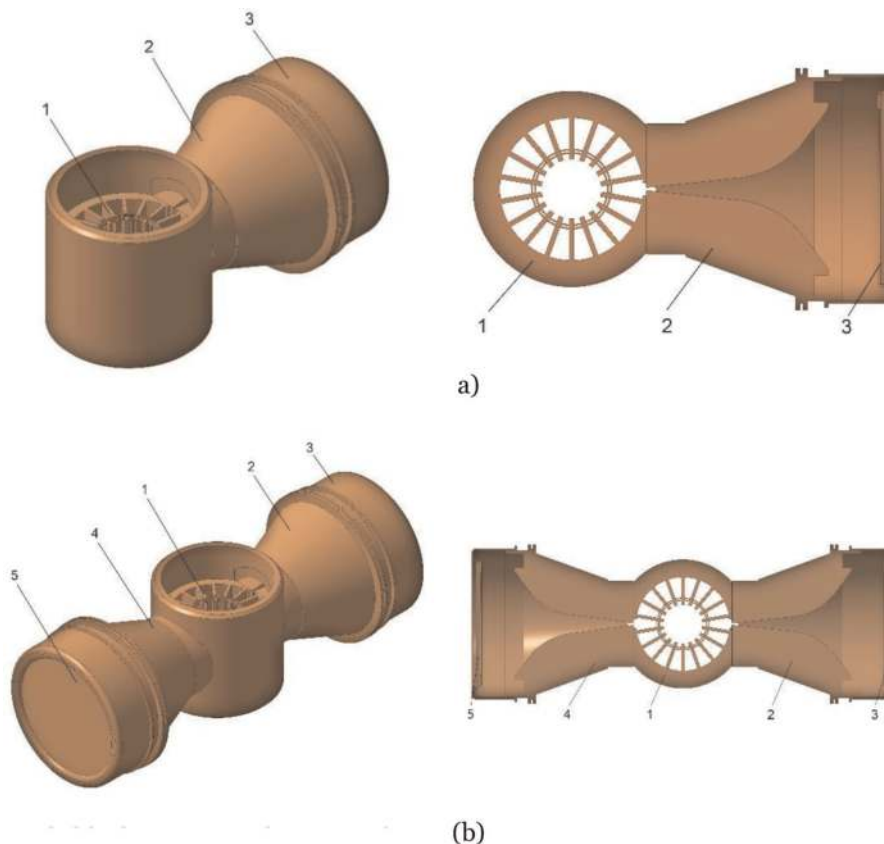


**Figure 13.** 3D images of a classical magnetron design (a) 1—an anode block; 2—a matching transformer; 3—a RF output of energy and a magnetron with two RF output of energy (b) 1—an anode block; 2—a matching transformer of an active RF output; 3—an active RF output of energy; 4—a matching transformer of an reactive RF output; 5—an active RF outputs of energy.

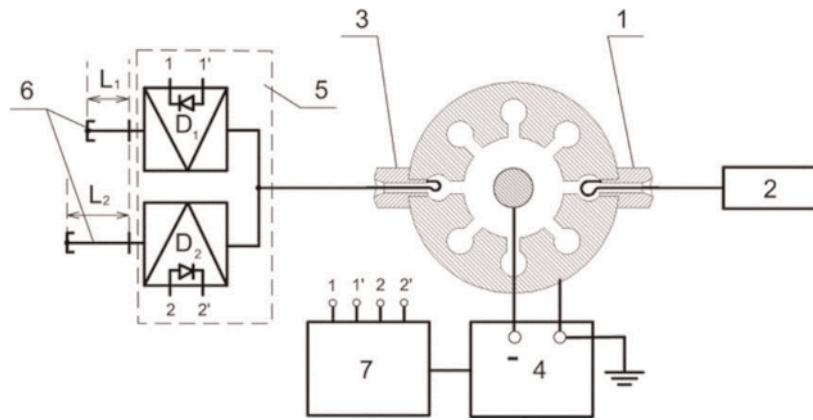


**Figure 14.**  
 A block diagram of the multifrequency magnetron generator [21, 38].

$L_i$ , where  $i = 1, 2, 3, \dots N$  (in our case,  $N = 2$ ). In the process, a value of  $N$  defines a number of frequencies generated by the magnetron, generally.

In recent years, there is a major interest in the creation of the high power microwave tubes and the electronic systems on its basis [9, 15, 16, 29, 33, 42]. An analysis shows that for getting the high power microwave radiation, there are several possible approaches based on:

- an application of the relativistic microwave devices (magnetron, vircator, gyrotron, etc.);
- a generation of short and ultra-short video pulses employing the high-voltage generators (for example, Marx's generator);
- an application of nonrelativistic microwave tubes (magnetrons) and temporal resonant compression of the microwave pulses;
- a forming of focused microwave beam by application of a phased array and a system of specially distributed emitters.

The vistas of creating the high-power microwave electronics are associated with developing the high-power relativistic microwave tubes, which are provided by generation of high-power microwave pulses (peak power is units and tens GW) [9, 33]. However, the application of such devices is connected with considerable technical and technological difficulties, especially, when need to produce a compact microwave electronic system generating very short microwave pulses (duration less 100 ns). In this case for forming high power microwave pulses, there are simpler approaches based on application both the high-voltage Marx's generator and the nonrelativistic microwave tubes (magnetrons). In the last case, we supported to apply the pulse compression technology, namely the resonant microwave compression method. A central idea of this method is slow storage of electromagnetic energy in the microwave resonator and then its removal from the high factor resonator for shorter duration to a matched load (antenna) [42]. Among advantages of this method, it is necessary to note its ease of its realization, the possibility of application the industrial magnetrons, as well as the standard elements of waveguide techniques. In our case, we consider an operation of the microwave module, in which the magnetron having the two RF outputs of energy is used.

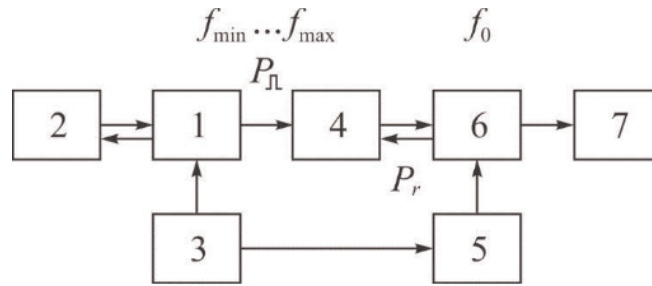


**Figure 15.** Block diagram of the high power microwave module [43]. 1—a magnetron with two RF outputs; 2—a tunable short-circuit waveguide; 3—a pulsed power supply (modulator); 4—ferrite isolator; 5—a generator of controlling pulses; 6—a microwave cavity; 7—a matched load (antenna).

**Figure 15** shows a block diagram of the microwave module for temporal compression of the microwave pulses and generates the high power microwave radio pulses [43]. The magnetron that is used in this experiment has an active and a passive RF output ports. To tune the frequency of the magnetron, we used the tunable short-circuit waveguide as the reactive load of the passive RF output. The result of the frequency tuning under changes of a position  $L$  of the short-circuiting piston at the reactive load of the magnetron was shown in **Figure 12**.

The analysis shows that application of the magnetron with two RF outputs in the microwave plant for forming the high power ultrashort microwave pulses allows increasing the efficiency of compression of the microwave pulses necessary to reduce a loss of power  $P_r$ , connected with possible reflection from microwave cavity 6 for reasons of availability of existing discrepancy between the resonant frequency of a microwave cavity  $f_0$  and a frequency of the magnetron. Assuming that  $f_{\min} < f_0 < f_{\max}$ , with the help of a short-circuiting piston, we adjust an oscillation frequency of the magnetron to a resonant frequency of the microwave cavity, and as a result, the power  $P_r$ , reflected from microwave cavity is decreased.

In **Figure 16**, the general view of universal block diagram of the plant for generating and forming a high power microwave radiation is shown. As we notice that the radiation can be presented either as sequence of short or super-short video

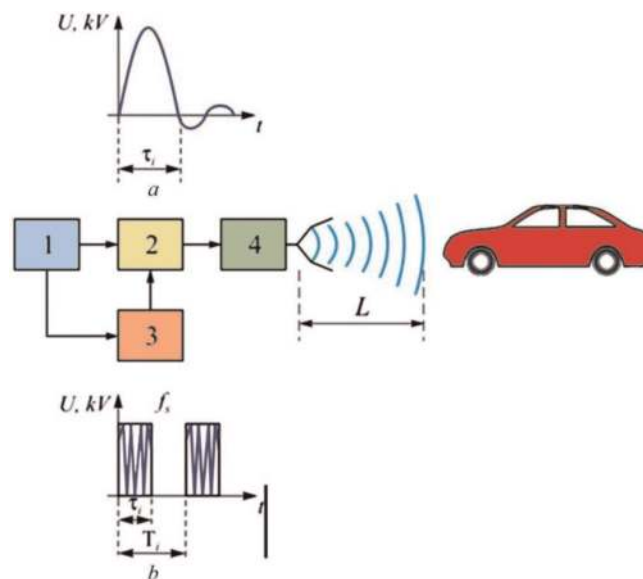


**Figure 16.** A block diagram of the high-power plant on basis of magnetron generator. 1—a source; 2—a microwave cavity; 3—a power supply; 4—antenna.



pulses (case of a), or it is considered as periodical sequence of the radio-frequency pulses (case of b).

Thus, the above-mentioned examples of applying the high power generators indicate that, to date, a great demand of high power sources in many areas does not raise doubts. Also, there is a great variety of problems; the solution of which opens some new trends in the application of the high power microwave generators and the given results allow considering the employment of new designs of the mm range magnetrons and expand areas of their application in a new way.

### 3. 320 GHz TWT

#### 3.1 General subjects and problems

The problem of development of the terahertz range is connected with the development of effective and compact vacuum microwave generators and amplifiers at the frequencies of 90, 220, 460, 670, 850, and 1030 GHz. TWTs are referred to as the tube, which provides the broadest band within the average power level and the most often applied in electronic systems to solve a variety of tasks in the field of communication, including space communication, probing the Earth's surface, as well as the objects of near and far space [44, 45].

The main complexity accompanying the process of producing TWT in the terahertz range consists in a contradiction between the need to combine the small size of tube interaction space (for example, the diameter of the drift channel of the delay line) and the high density of the current of an electron beam. Considering the fact that the geometrical sizes of a tube decrease in proportion to the wavelength, i.e.,  $D \sim \lambda$ , where  $D$ — is the conventional size of tube interaction space and  $\lambda$ — is the wavelength in a free space, and there arise difficulties in passing an electron beam through the drift channel of the delay line. In certain cases, the given difficulties make the production of the delay line technologically impossible while applying the well-known methods and technologies. In general, these difficulties are purely technological, and they are connected not only with manufacturing the components of a tube construction (a delay line, an electron-optical system, an RF input and RF output devices, a collector, a magnetic-focusing system, etc.) but also with an assembly process of all its construction as a whole. Special consideration should be taken to the problems of providing the required critical dimensional features ( $\sim 1$ – $3$  microns) and surface finish (roughness) of the internal surface of the delay line ( $\sim 25$ – $30$  microns). The applied traditional technological production operations have limited opportunities already at the frequencies exceeding 400–450 GHz [46]. The specified technological difficulties have risen a considerable interest in employing programs of 3-D computer modeling of nonlinear processes of electron-wave interaction, including modeling of thermal processes in the tubes of the terahertz range. The application of the 3-D computer modeling allows defining the potentialities of the developed constructions already at the stage of tube designing in terms of ensuring the required level of power output that enables to considerably reduce the price and accelerate the development of devices as a whole.

A broad spectrum of problems accompanying the process of TWT creation in the terahertz range has led to the creation of various programs and even some new independent directions of the development of vacuum electronics in the world. First of all, it concerns a dynamically developing industry of integral vacuum microwave microelectronics, namely vacuum microelectronics of millimeter and terahertz ranges. In order to coordinate and combine the efforts of the companies which are engaged in the development of devices in the terahertz range, there have been special

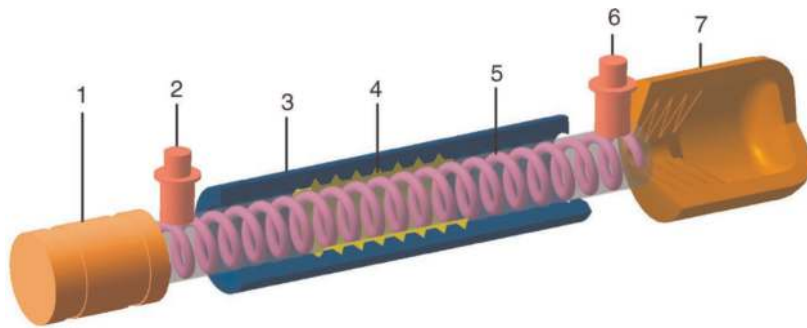


**Figure 17.** Scheme of the TWT design with the helix delay line. 1—an electron-optical system; 2—a RF input; 3—a magnetic focusing system; 4—a local absorber; 5—a helix-type delay line; 6—a RF output; 7—a collector.

programs for developing terahertz technologies. In the near-term outlook, it assures a substantial progress in the field of design and development of microwave devices in a short-wave part of the terahertz range.

### 3.2 The fundamentals of TWT operation physics

The general structure scheme of classical TWT is presented in **Figure 17**. An electron beam produced by the electron-optical system 1, which includes the electron gun, accelerating and focusing electrodes, passes the delay line 5, and precipitates on the collector 7. The tube input 2 is given a RF signal, which is amplified, and output through the output 6 into matched load. In order to prevent self-excitation of the TWT in a tube between RF input and RF output, there is the energy absorber 4, the main objective of which is to reduce the wave amplitude reflected from the output 6.

One of the TWT most complex nodes is the delay line. The helix delay lines have mostly become wide spread in average power level TWT's of the centimeter and millimeter ranges. As the analysis reveals, the reduction of wavelength results in a considerable decrease in the efficiency of interaction in these systems (the value of coupling impedance decreases to a few Ohms and less), as well as some difficulties connected with the production of wire for a helix whose diameter becomes less than 50 microns. Because of this, it is necessary to have alternative types of the delay lines, which would possess acceptable electrodynamic characteristics and the ability to pass electron beams with necessary current density. In addition, these structures have to meet the demands of production simplicity while preserving thermal stability and a possibility to withdraw heat energy from its structural elements, mechanical durability, and the ability to withstand a load of various external factors (temperatures, vibrations, accelerations, etc.). It is also essential to consider that the limiting values of the dimensions of the delay lines depend on the peculiarities of their design. For this reason, the helix delay lines can be used at the frequencies, which do not exceed 60–65 GHz [47].

The analysis of publications of the last 10 years reveals that there are a number of constructions of delay lines with dimensions, which are technologically implementable in the terahertz range involving a folded waveguide, a dual comb with different types of excitation, and metal film structures on dielectric bases. In recent years, due to the extreme complexity of manufacturing in the terahertz range, classical miniature resonators and delay lines photonic crystals have been proposed to be used as delay lines [48, 49].

The existing delay lines have an essential shortcoming connected with the fact that the electromagnetic wave in these devices is surface wave, and a longitudinal z-component of an electromagnetic field, the electron beam interacting with it,

decreases from the outline border of the delay line to its axis. Therefore, a great interest is the microwave plasma-filled tubes with Cherenkov's radiation mechanism in which the electromagnetic wave is volumetric [50]. As a result, efficiency of interaction process between electron beam and electromagnetic wave is raised. It leads to increasing output power in such tubes.

**Figure 18** schematically presents the design of plasma TWT. The presence of plasma allows to considerably increase the width of frequency range, to raise the output power and interaction efficiency and also enables the operational control of frequency range by implementation of tube frequency tuning both from an pulse to an pulse and within an microwave pulse. However, in order to implement the tubes for practical purposes, it is necessary to carry out additional investigations on some of unsolved problems which are related to features of beam-plasma interaction in these tubes.

### 3.3 3-D computer modeling results

As an example, let us consider the 3-D computer modeling of a delay line for TWT at the frequency of 320 GHz. As the delay line, the folded waveguide was taken, one period of which is shown in **Figure 19**. The main dimensions of the folded waveguide are presented in **Table 4**.

It is necessary to note that the folded waveguides are the most popular ones, and they are often applied to design TWT in the range up to 400 GHz due to the compact dimension, broad band, and ease in production using, for example, the UV LIGO or MEMS technologies [51–53].

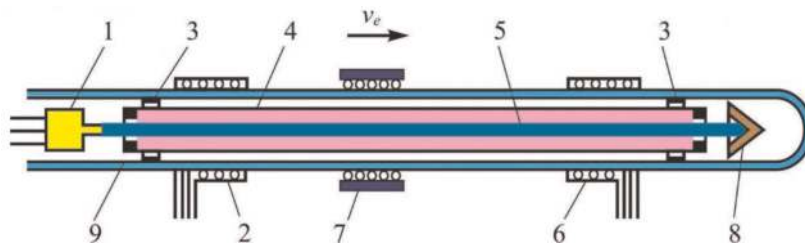


**Figure 18.** Scheme of plasma TWT. 1—an electron-optical system; 2—a RF input; 3—plasma ignition device; 4—plasma; 5—an electron beam; 6—a RF output; 7—an absorber; 8—a collector; 9—a bulb [50].

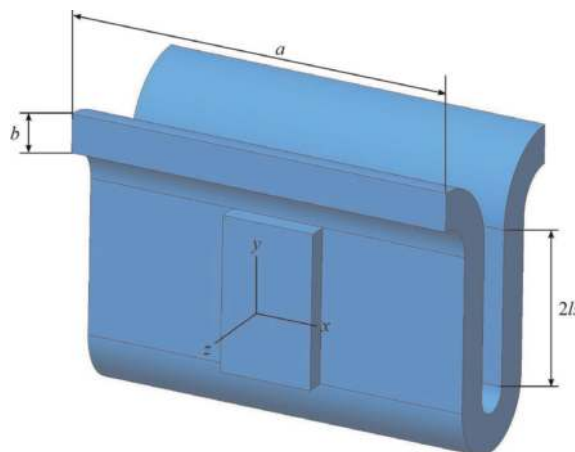


**Figure 19.** Illustration of one period of a folded waveguide.

Parameter	Symbol	Value
1. Wide wall of waveguide, mm	a	0.6
2. Narrow wall of waveguide, mm	b	0.09
3. Pitch (one half of structure period), mm	p	0.18
4. One half of length of straight part of waveguide, mm	ls	0.125

**Table 4.**  
Parameters of a folded waveguide.

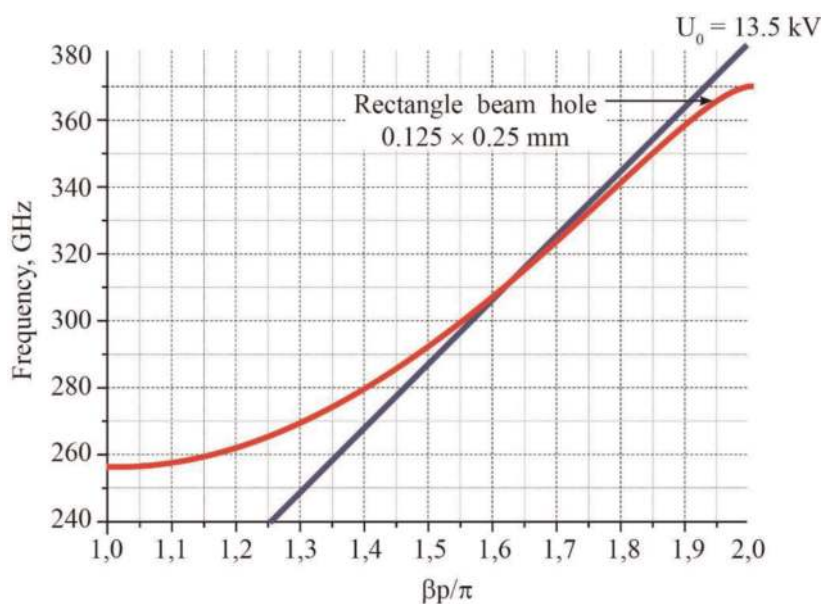


**Figure 20.**  
A dispersion diagram in case of the rectangular hole for electron beam (a red curve) and electron beam voltage (a blue curve).

The results of computer modeling present in **Figure 20**. In this figure, a dispersion diagram and electron beam voltage are shown. As you have seen, the intersection of the curves determines an operating mode of a tube. A maximum amplification band corresponds to rectangular hole for electron beam (see **Figure 20**) whose dimensions are  $0.125 \times 0.25$  mm. An electron beam voltage is equal 13.5 kV.

#### 4. Conclusion

The current status of the theory of electron-wave interaction in a 3-mm magnetron using the mode other than  $\pi$ - mode (the so-called surface-wave magnetron) and the design of the magnetron with two RF outputs are considered. It is shown that a process of phase focusing an electron beam in interaction space of the surface wave magnetron (interaction with  $-1$  space harmonic) has a feature connected with concentration of energy of RF wave in the vicinity of a surface of the anode block. In this case for effective interaction between electron beam and RF wave, it is necessary to raise a height of electron hub of space charge in comparison with, for example, the classical magnetron. New data directed to improving the frequency characteristics of magnetrons and expanding their functionality for application in various electronic systems are obtained. In particular, the application of a pulse 2-cm magnetron with two RF outputs allows

realizing a mode of electronic frequency tuning from pulse to pulse in the range 200–300 MHz. As a result of improving the frequency characteristics of magnetron generators, new circuitry was proposed for creating various electronic systems in which these magnetrons can be used.

The trend in the progress of the TWT design in the terahertz frequency range has been analyzed. Using as an example of 3-D computer modeling of a slow-wave structure as a folded waveguide, the principal possibility of designing a TWT at a frequency of 320 GHz is presented. It is shown that the advancement in the short-wave part of the terahertz range is largely associated with the search and implementation of new efficient designs of the main components of the TWT's and the slow-wave structures.

## Acknowledgements

The authors would like to thank Prof. Ye. Odarenko and Dr. V. Gerasimov for helpful discussions and numerical calculations as well as Assistance Prof. T. Frolova and Mrs. E. Isaeva for help in preparing the manuscript.

## Author details

Gennadiy Churyumov<sup>1</sup>, Jinghui Qiu<sup>2</sup> and Nannan Wang<sup>2\*</sup>


<sup>1</sup> Kharkiv National University of Radio Electronics, Kharkiv, Ukraine

<sup>2</sup> Harbin Institute of Technology, Harbin, China

\*Address all correspondence to: [wangnn@hit.edu.cn](mailto:wangnn@hit.edu.cn)

## IntechOpen

---

© 2019 The Author(s). Licensee IntechOpen. This chapter is distributed under the terms of the Creative Commons Attribution License (<http://creativecommons.org/licenses/by/3.0>), which permits unrestricted use, distribution, and reproduction in any medium, provided the original work is properly cited. 

## References

- [1] Cherenkov PA. Visible emission of clean liquids by action of  $\gamma$  radiation. *Doklady Akademii Nauk SSSR*. 1934;**2**: 451. Reprinted in selected papers of soviet physicists, *Usp. Fiz. Nauk* 93, 385, (1967)
- [2] Tamm IE, Frank IM. Coherent radiation of fast electrons in a medium. *Doklady Akademii Nauk SSSR*. 1937;**14**: 10 (in Russian)
- [3] Jelle JV. Cerenkov radiation and its applications. *British Journal of Applied Physics*. 1955;**6**:277
- [4] Bolotovskii BM. Vavilov-Cherenkov radiation: Its discovery and application. *Physics-USpekhi*. 2009;**52**(11): 1099-1110. (in Russian)
- [5] Smith SJ, Purcell HM. Visible light from localized surface charges moving across a grating. *Physics Review*. 1953; **92**:1069-1070
- [6] Elder FR, Gurewitsch AM, Langmuir RV, Pollock HC. Radiation from electrons in a synchrotron. *Physical Review*. 1947;**71**(11):829-830
- [7] Potylitsyn AP, Ryazanov MI, Strikhanov MN, Tishchenko AA. Diffraction radiation from relativistic particles. *Springer Tracts in Modern Physics*. 2011;**239**:1
- [8] Ter-Mikaelyan ML. Influence of Medium on Electromagnetic Processes Under High Energies. Erevan: AS of Arm. SSR; 1969. p. 459. (in Russian)
- [9] Gilmour AS Jr. Klystrons, Traveling Wave Tubes, Magnetrons, Crossed-Field Amplifiers, and Gyrotrons. Boston, MA: Artech House Inc, 2011. 883 p
- [10] Proceedings of the 11-th International Vacuum Electronics Conference (IVEC 2010); 2010
- [11] Dicke RH. Coherence in spontaneous radiation processes. *Physics Review*. 1954;**93**:99-110
- [12] Hull AW. The effect of a uniform magnetic field on the motion of electrons between co-axial cylinders. *Physics Review*. 1921;**18**(1):13
- [13] Fisk JB, Hagstrum HD, Hartman PL. The magnetron as a generator of Centimeter waves. *The Bell System Technical Journal*. 1946;**25**(2):167-348
- [14] Collins GB. *Microwave Magnetrons*. New York: McGraw-Hill; 1948
- [15] Military Critical Technology List. Section 8: Electronics Technology: Undersecretary of Defense, Acquisition, Technology and Logistics. USA: Pentagon; 2006. pp. 1-108
- [16] Osepchuk JM. Microwave power applications. *IEEE Transactions MTT*. 2002;**50**(3):975-985
- [17] Okress EC, editor. *Microwave Power Engineering*. Vol. 1, 2. New-York & London: Academic Press; 1968
- [18] Edgar RH. In: Edgar RH, Osepchuk JM, editors. *Consumer, Commercial, and Industrial Microwave Ovens and Heating Systems*. New York: Marcel Dekker; 2001. pp. 215-278
- [19] Shinohara N. Development of active phased array with phase-controlled magnetrons. In: Shinohara N, Fujiwara J, Matsumoto H, editors. *International Symposium on Antennas and Propagation: Int. Conf*, 21–25 Aug. Vol. 2. Fukuoka, Japan; 2000. pp. 713-716
- [20] Brown WC. Satellite power system (SPS) magnetron tube assessment study. W. C. Brown. NASA Contract NAS-8-33157 for MSFC; July 10, 1980

- [21] Churyumov GI, Gerasimov VP, Frolova TI, et al. The advanced designs of magnetrons with improvement output characteristics. 17th International Vacuum Electronics Conference (IVEC 2016), (19–21 April 2016 Monterey, California); 2016
- [22] JSC “RPC “Istok” <http://istokmw.ru/index.php?lang=en>
- [23] Churyumov GI, Ekezli AI. The Anomalous Increasing of the Anode Current in the Diode Structures. 17th International Vacuum Electronics Conference (IVEC 2016); (19–21 April 2016 Monterey, California); 2016
- [24] JSC “Pluton” <http://pluton.msk.ru/en/>
- [25] CPI <https://www.cpii.com/division.cfm/1>
- [26] Nation JA et al. Advances in cold cathode physics and technology. Proceedings of the IEEE: Special Issue – New Vistas for Vacuum Electronics. 1999;87(5):865-889
- [27] Ayzatskiy NI, Churyumov GI, Dovbnaya AN, et al. Generation and formation of axially-symmetrical tubular electron beam in a cold metal secondary-emission cathode magnetron gun – Part I: Experiment. IEEE Transactions on Electron Devices. 2016; 63(4):1704-1709
- [28] Ayzatskiy NI, Churyumov GI, Dovbnaya AN, et al. Generation and formation of axially-symmetrical tubular Electron beam in a cold metal secondary-emission cathode magnetron gun – Part II: Computer modelling. IEEE Transactions on Electron Devices. 2016; 63(4):1710-1714
- [29] Patent of Russia, No 2356065. The Nanosecond Radar Method Using Pulse Compression Resonance from Transmitter. Novikov SA, et al. Zayavl. 08.05.2007 (in Russian)
- [30] Truten ID et al. The millimeter pulsed magnetrons using the mode of spatial harmonics. UPHJ. 1975;20(7): 1170-1176. (in Russian)
- [31] Usikov AY, editor. Electronics and Radio Physics of Millimeter and Submillimeter Waves. Kiev: Naukova dumka; 1986. 386 p. (in Russian)
- [32] Slutskin AA. The mechanism of excitation of oscillations in multi-segment magnetrons. JTPH. 1947;XVII (4):425-434 in Russian
- [33] Magda II, Gadetski NP, Kravtsova EI, et al. Relativistic magnetron of millimeter waveband. In Proc. 18th IEEE Int. Crimean Conf. Microw. Telecommun. Technol., Sevastopol', Ukraine; 2008. pp. 637-639
- [34] Churyumov GI et al. The multiperiod mathematical model of the magnetron. Radio Electronics and Informatics. 2006;2:15-27. (in Russian)
- [35] Imran Tahir, M. Frequency and Phase Locking of a CW Magnetron (with a digital phase locked loop using pushing characteristics). Thesis. Lancaster University; September 2008. 204 p
- [36] Obata H, Tsuji N, Furumoto K. Electronic-frequency-tuning magnetron. IEEE Transactions on Electron Devices. 2012;59(11):3111-3115
- [37] Churyumov GI. The Qualitative Theory of Electron Beam Formation in a Surface Wave Magnetron (Invited Talk) 9th International Kharkiv Symposium on Physics and Engineering of Microwaves, Millimeter and Sub-Millimeter Waves (MSMW 2016), Kharkiv (Ukraine), 21-24 June, 2016. pp. 112-114
- [38] Churyumov GI, Ekezli AI. Frequency tuning from pulse to pulse

- magnetron generator. Patent of Ukraine # 98574, 2010 (in Ukraine)
- [39] Churyumov GI, Ekezi AI. Investigation of the regime of frequency tuning in a pulsed magnetron with two outputs of energy. *Elektronnaya Technika, Ser. 1, SVCh-Technika*. 2014; 2(521):39-45. (in Russian)
- [40] Special Issue on New Vistas for Vacuum Electronics. *Proceedings of the IEEE*. 1999;87(5):935
- [41] Shlifer ED. Calculation of Multiresonator Magnetrons. 2nd ed). M.: MEI1966. 142 p. (in Russian)
- [42] Benford J, Swegle JA, Schamiloglu E. *High Power Microwaves*. 2nd ed. CRC Press; 2007. 556 p
- [43] Churyumov GI. High-power microwave electronics: Current status, prospects of development and application features. *Applied Radio Electronics*. 2013;15(4):270-300. (in Russian)
- [44] *Proceedings of the 11th IEEE International Vacuum Electronics Conference (IVEC'2010)*; 2010
- [45] Song H-J, Nagatsuma T, editors. *Handbook of Terahertz Technologies Devices and Application*. CRC Press; Pan Stanford Publishing; 2015. 582 p
- [46] Ponomarenko SS, Kishko SA, Zavertanniy VV, et al. 400-GHz continuous-wave Clinotron oscillator. *IEEE Transactions on Plasma Science*. 2013;41(1):82-86
- [47] Bushuev NA. The problem of development of the wide-band mm and sub-mm range TWTO. *Journal of Radio Electronics*. 2016;11:1-21. (ISSN 1684-1719) (in Russian)
- [48] Letizia R, Mineo M, Paoloni C. Photonic crystal-structures for THz vacuum Electron devices. *IEEE Transactions on Electron Devices*. 2014; 62(1):178-183
- [49] Odarenko EN. Photonic crystal waveguide structures for terahertz band electronic devices. *Telecommunications and Radio Engineering*. 2015;74(3): 221-230
- [50] Bernashevskiy GA, Bogdanov YB, Kislov VY, Chernov ZS. *Plasma and Electronic Microwave Amplifiers and Generators*. – M.: Izd-vo “Sovetskoye Radio”. 1965. 95 p. (in Russian)
- [51] Goldenberg BG et al., editors. *Fabrication of microstructured optical elements for visible light by means of LIGA-technology*. In: *Nuclear Instruments & Methods in Physics Research. Sec. A*. 2009;603(1/2) *Proceedings of the XVII International Synchrotron Radiation conference: SR-2008, Novosibirsk, Russia, June 15–20. 2008*. pp. 157-159
- [52] *MEMS and MOEMS Technology and Applications (SPIE Press Monograph Vol. PM85)* by P. Rai-Choudhury; 2000. 516 p
- [53] Tsutaki K, Neo Y, Mimura H, et al. Design on a 300 GHz band TWT with a folded waveguide fabricated by microelectromechanical systems. *Journal of Infrared, Millimeter, and Terahertz Waves*. 2016. DOI: 10. 1007/s10762-016-0306-5